MONTE CARLO STUDY OF DILUTE SOLUTIONS OF HETEROARM STAR COPOLYMERS IN SOLVENTS DIFFERING IN THERMODYNAMIC QUALITY

Jitka HAVRÁNKOVÁ[1], Zuzana LIMPOUCHOVÁ[2] and Karel PROCHÁZKA[3,*]

Department of Physical and Macromolecular Chemistry and Laboratory of Specialty Polymers, Faculty of Science, Charles University, Albertov 6, 128 43 Prague 2, Czech Republic; e-mail: [1] jh@vivien.natur.cuni.cz, [2] zl@vivien.natur.cuni.cz, [3] prochaz@vivien.natur.cuni.cz

Received July 1, 2005
Accepted September 26, 2005

Dedicated to our great friend and colleague Dr. Marta Pacovská who left us for ever a year ago.

Lattice Monte Carlo simulations (an original modification of the Siepmann and Frenkel simulation variant) was used to study the conformational behavior of heteroarm star copolymers star-(polystyrene; polyisoprene), PS_8PI_8, in a common good solvent for both types of arms (tetrahydrofuran) and in selective θ-solvents for both types of arms (in cyclohexane, i.e., in θ-solvent for PS and in 1,4-dioxane, i.e. in θ-solvent for PI). Results of simulations were compared with experimental data published by Pispas et al. The coarse graining procedure was performed to match the experimental behavior of heteroarm stars in a good solvent. The computer simulations reproduce all decisive trends of the conformational behavior for both selective solvents. The quantitative agreement between experimental and simulated size characteristics is very good. Simulations yield very detailed information on the system at the molecular level and show that the incompatible arms significantly segregate in selective solvents.

Keywords: Monte Carlo simulations; Siepmann and Frenkel simulation; Conformational behavior; Polymers; Star copolymers; Solvent effects; Dynamics.

Computer simulations are very important tool for studying dynamics, conformational behavior, properties and phase diagrams of polymer systems. Nowadays Monte Carlo and molecular dynamics methods have become an indispensable part of polymer research. Great achievements in computer technology in recent decades together with development and optimization of new efficient simulation algorithms made computer studies of very complex polymer systems possible. The up-to-date simulations cover very broad range of scientific topics associated with polymers, ranging from studies of important biopolymers on one hand (e.g., DNA, proteins and

peptides)[1–3] through a very large field of specific polymer properties (e.g., chains in solutions, in pores and at interfaces)[4–7] to the research topics concerning self-assembled polymeric nanoparticles on the other[8–11]. We have been using lattice Monte Carlo methods for studying properties of self-assembled polymer systems (polymeric micelles with kinetically frozen cores) for more than one decade[12–18]. Recently we developed an efficient simulation variant for studying conformations of homo- and heteroarm star polymers. We have described individual simulation steps and presented the most important characteristics together with general trends of the behavior of dilute solutions of heteroarm stars in our earlier publication[14].

In this communication, we compare new results of Monte Carlo simulations with experimental data on heteroarm copolymers published by Pispas et al. some time ago[19]. Heteroarm copolymer are an important class of polymeric materials. Their most decisive properties are similar to those of linear di- and triblock copolymers rather than to multiblock copolymers. They form microphase-segregated structures in the melt and self-assembled nanoparticles in solutions in selective solvents[20–22]; however, their behavior differs in a number of details from that of linear block copolymers. For example, upon dissolution in selective organic solvents, they form spontaneously reversible micelles, but the association number is lower and the critical micelle concentration is higher compared with linear copolymers of the same overall composition[21]. The star architecture promotes solubility in selective solvents and "hairy" heteroarm star copolymers (containing high numbers of both soluble and insoluble arms) may survive in a mild selective solvent in unimer form because their conformations with expanded soluble blocks and partially collapsed insoluble blocks remind spherical multimolecular micelles formed by a number of diblock chains[22].

The aim of the paper is the following: We want to demonstrate that the relatively simple lattice Monte Carlo simulations are able to reproduce the experimentally observed behavior of star copolymers very well. We want to show that computer simulations help to understand their behavior at the molecular level and to explain and predict all main trends.

SIMULATION METHOD

The simulation method used in this work was described in detail in our recent papers[14] Here we briefly summarize the most important steps. The program generates random conformations of star copolymers A_8B_8 with two types of arms (poorly soluble A and well-soluble B arms) on a simple cubic lattice with the spacing l_C. A rectangular simulation box is composed

of 100 × 100 × 100 lattice points and contains one star copolymer only. Periodic boundary conditions are applied in all three directions. The center of the star is located in the center of the simulation box.

An original variant of the configuration-bias (fully ergodic and microscopically reversible) equilibration algorithm similar to that of Siepmann and Frenkel[23] is applied to get equilibrated conformations. It consists of the following steps:

1. A bead (*j*) of an arm (*k*) is chosen at random.

2. The part of the *k*-th arm from the *j*-th bead (inclusive) to the end bead is erased and its Rosenbluth weight[24], W_{old}, is calculated in the following way: The end bead is erased first and its weight contribution is calculated using the formula

$$w_{\text{N}} = \sum_{l} \exp(-U_l/kT) \,. \qquad (1)$$

The sum applies for all free lattice sites, *l*, around the (*N* – 1)-st bead, U_l is the interaction energy of the *N*-th bead in the position *l* (calculated as the sum of pair interactions u_{ij} of the *N*-th bead with neighboring lattice sites), *k* is the Boltzmann constant and *T* is temperature. The potential energy U_l of a bead in position *l* depends only on the nearest lattice neighbors. Other beads (up to *j* + 1) are deleted one by one and weights w_i are calculated using Eq. (*1*). The weight of the *j*-th bead is $w_j = \exp(-U_j/kT)$. The total Rosenbluth weight W_{old} is given by the product of individual contributions w_i

$$W_{\text{old}} = \prod_{i=j}^{N} w_i \qquad (2)$$

3. A new conformation of the reconstructed part of the arm *k* is generated by the following configuration-bias procedure. First, the position of the *j*-th bead is chosen at random and its weight is calculated $w_j = \exp(-U_j/kT)$. The bead to be placed next may be located in *l* different positions. Because the interaction energy differs for different positions *l*, the a priori probabilities for a random selection of individual positions *l*′ are calculated using the formula

$$P_{l'} = \frac{\exp(-U_{l'}/kT)}{\sum_{l} \exp(-U_l/kT)} \qquad (3)$$

where $w_j = \sum_l \exp(-U_l/kT)$ is the new weight of the *j*-th bead. Then the self-avoiding growth of the part that was deleted in the previous step continues until the arm is completed. The a priori probabilities are evaluated by

means of Eq. (*3*), the Rosenbluth weights of beads, w_j, and the total weight of the new part of the arm, W_{new}, are calculated using Eqs (*1*) and (*2*), respectively.

4. A modified acceptance criterion of the Metropolis type is used to accept/reject the new conformation of the randomly erased and reconstructed part of the arm[25].

$$\text{rand}(0;1) \leq \frac{W_{new}}{W_{old}} \qquad (4)$$

CALCULATED FUNCTIONS

In our previous papers, we defined a number of structural characteristics of the heteroarm star and characteristics of both types of arms that quantify the conformations and describe the behavior of the system. We calculate two types of characteristics: (i) mean values of selected distances (average end-to-end distance and others) and (ii) various distribution functions. Since the Monte Carlo technique generates a high number of statistically independent conformations, both types of characteristics may be readily evaluated. Individual distribution functions are constructed as histograms in simulations. In this study, we concentrate on selected characteristics that were measured experimentally by Pispas et al., i.e., on the overall size characteristics. We calculated also other functions such as the distribution of end-to-end distances for both types of arms, $\rho_{EE}(R_A)$ and $\rho_{EE}(R_B)$, i.e., distribution functions of end distances from the center of the star, functions averaged for n arms of a given type. However, we do not present all these functions in this communication (they are available upon request).

The calculated and discussed distribution functions are the distributions of radii of gyration. We evaluate the distribution function of the gyration radii of the whole star, $\rho_G(R_G)$ and distributions of gyration radii of all segments of a given type, $\rho_g(R_{gA})$ and $\rho_g(R_{gB})$.

Since very useful information on the spatial distribution of segments A and B can be obtained from evaluating the distance between the gravity centers of different types of arms, we calculated distribution functions of distances of gravity centers of all segments A and of all segments B from the geometrical center (the branch point) of the star $\rho_{TA}(r)$ and $\rho_{TB}(r)$, respectively. Since the positions of gravity centers T(A) and T(B) do not have to coincide with lattice points, these functions are not normalized by the numbers of lattice points, but by the volumes of narrow spherical layers of thickness Δr.

EXPERIMENTALLY STUDIED SYSTEM

In this paper we address the conformational behavior of two coarse-grained heteroarm systems that correspond to two systems of star-(polystyrene; polyisoprene), PS_8PI_8, heteroarms with $M_w = 3.3 \times 10^5$ and 7.1×10^5 g/mol studied experimentally by Pispas et al.[19] in tetrahydrofuran (common good solvent for both types of arms), in cyclohexane (θ-solvent for PS) and in 1,4-dioxane (θ-solvent for PI). These authors synthesized and characterized several well-defined heteroarm star copolymers with the same number and almost the same molar mass of two types of arms and studied their solution behavior in solvents differing in thermodynamic quality and selectivity as a function of their overall molar mass (i.e., the lengths of arms) by viscometry and light scattering. The reported hydrodynamic radii, R_H, they obtained by dynamic light scattering measurements, can be easily compared with results of our simulations.

PARAMETERS OF THE STUDIED SYSTEM

In our simulations, we use a simple set of pair interaction parameters that are currently used in lattice simulations for block copolymers in selective solvents. The interaction of polymer segments with the solvent is modeled indirectly via effective interactions between segments (expressing the difference between interaction of a segment with an other segment or with solvent, similarly to the Flory–Huggins approach), i.e., all pair interaction parameters with the solvent equal zero, $u_{AS} = u_{BS} = u_{SS} = 0$. For interactions between beads of the same type in a common good solvent, $u_{AA} = u_{BB} = 0$. In a selective solvent for one of blocks, either u_{AA}/kT, or u_{BB}/kT equals –0.27, which corresponds to current definition of the θ-state for the pertinent block (the remaining parameter is zero). The parameter u_{AB} was obtained using a parametrization procedure as described bellow.

In order to compare experimental and simulated data quantitatively (not only qualitative trends) special attention had to be paid to the coarse graining and back mapping. An appropriate value of the lattice constant, l_C, an appropriate number of the "Kuhn lattice segments" and the value of interaction parameter $u_{AB}/kT = 0.12$ were obtained by comparing the simulated contour lengths of arms and simulated radii of gyration of the two homostar copolymers in an athermal solvent with experimental values. Because we need to obtain "universal" parameters that describe both experimental systems well, we use the following criteria for the goodness of the fit

$$S^2 = \frac{(R_{G1}^{sim} - R_{G1}^{exp})^2}{\sigma_{sim1}^2(R_{G1}^{sim}) + \sigma_{exp1}^2(R_{G1}^{exp})} + \frac{(R_{G2}^{sim} - R_{G2}^{exp})^2}{\sigma_{sim2}^2(R_{G2}^{sim}) + \sigma_{exp2}^2(R_{G2}^{exp})} \quad (5)$$

where subscripts 1 and 2 refer to the experimentally studied systems S1 and S2 and superscript/subscripts sim and exp refer to results of our simulations and experimental work by Pispas, respectively. The scatter in experimental values is taken from ref.[19] and simulations provide directly the second moment of pertinent distribution functions. The positive u_{AB}/kT value reflects the incompatibility of PS and PI arms. Since simulations yield directly the radius of gyration, R_G, while in experiments hydrodynamic radii, R_H, are easier accessible quantities than R_G and values of R_H were published by Pispas, we used the recalculation formula, $R_H/R_G = 0.77$ which holds in good solvents[26].

The used characteristics of the experimentally studied systems are listed in Table I and the characteristics of coarse-grained model systems are listed in Table II. Interaction parameters that model common good solvents and θ-solvents for individual blocks are given in Table III.

TABLE I
Characteristics of the experimentally studied star systems

Star copolymer	$M_{w,star} \times 10^{-5}$	$M_{w,PS} \times 10^{-4}$	$M_{w,PI} \times 10^{-4}$	$N_{MU,PS}$	$N_{MU,PI}$	L_{PS}	L_{PI}
S1	3.30	2.09	2.02	200	300	50	124
S2	7.10	4.36	4.82	420	710	105	293

$M_{w,star}$, molar mass of the whole star; $M_{wPS(PI)}$, molar mass of one PS (PI) arm; $N_{MU,PS(PI)}$, number of monomer units of PS (PI) arm; $L_{PS(PI)}$, contour length of PS (PI) arm.

TABLE II
Characteristics of coarse-grained model systems

Star copolymer	l_c, nm	n_A	n_B
S1	1.8	28	69
S2	1.8	57	163

l_c, lattice constant; n_A (n_B), number of Monte Carlo segments.

RESULTS AND DISCUSSION

In order to compare our results with available experimental data, we focus mainly on the size characteristic, i.e., on radii of gyration. Figure 1 shows distribution functions of radii of gyration of individual blocks for heteroarm stars S2 in all three solvents. As pointed out by Pispas, heteroarm stars are expanded in a common good solvent for both blocks relatively to the size of corresponding homoarm stars (with the same total number of arms of the same type, i.e., in this case with 8 longer and 8 shorter arms of the same composition) as a result of incompatibility of PS and PI blocks. The

TABLE III
Interaction parameters that model a common good and θ-solvents for individual blocks

Solvent	u_{AA}, kT	u_{BB}, kT	u_{AB}, kT
Common good solvent	0	0	0.12
θ-solvent for PS, good for PI	–0.27	0	0.12
θ-solvent for PI, good for PS	0	–0.27	0.12

u_{BB}, interaction parameter between segments B; u_{AA}, interaction parameter between segments A; u_{AB}, interaction parameter between different segments.

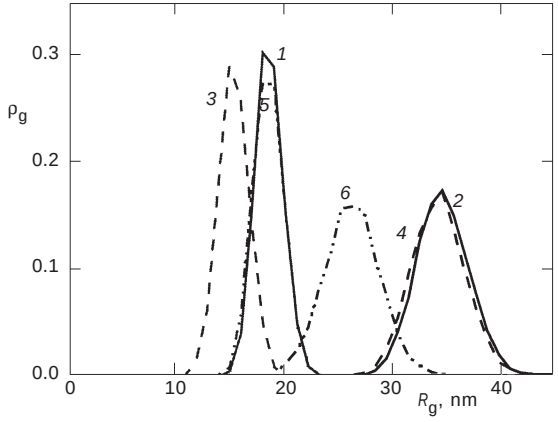

FIG. 1
Distribution functions, ρ_g of radii of gyration of PS and PI arms ($R_{g,sim,PS}$ and $R_{g,sim,PI}$, respectively) in star-(polystyrene; polyisoprene), PS_8PI_8, S2. Solid curves *1* and *2* correspond to PS and PI arms in a common good solvent (tetrahydrofuran), dashed curves *3* and *4* correspond to the θ-solvent for PS and a good solvent for PI (cyclohexane) and dashed dot dot curves *5* and *6* correspond to a good solvent for PS and the θ-solvent for PI (1,4-dioxane)

curve for coarse-grained homostar (i.e., for $u_{AB} = 0$) is not shown to prevent overcrowding of the figure. When comparing absolute values on the R_G scale, the following must be taken into account. In both experimental systems S1 and S2, the molar masses of both types of arms are comparable, but the relative molecular weight of the PS monomer unit (M = 105) is significantly higher than that of PI (M = 68). Further, the flexibility of real PI chains is higher than that of PS chains and the number of monomer units forming one "lattice Kuhn segment" is lower, ca. 4.4 for PI and ca. 7.4 for PS. This results in almost three times longer PI arms compared with PS arms in our model calculations. Nevertheless, it is necessary to stress that the used coarse graining and subsequent simulation yield values quantitatively comparable with experimental values (if accessible) for both blocks. Full lines *1* and *2* depict the distribution of gyration radii of PS and PI arms in a common good (i.e., athermal) solvent, respectively. Both curves are almost symmetrical. That for PS (curve *1*) is narrower, a maximum around 18 nm and the broader one with a maximum around 35 nm (curve *2*) corresponds to PI. In cyclohexane (θ-solvent for PS), PS arms shrink (broken line *3*) and the maximum shifts to ca. 15 nm. Because the concentration of PS segments is low at longer distances from the gravity center, i.e., at the distances, where many PI segments are located, the incompatibility effect becomes less important, the PI arms relax and the distribution of radii of gyrations shifts to lower values. However, the observed shift is very small because it is partly compensated by the expansion of central parts of PI arms, which are being expelled from the central region due to increased concentration of PS segments. The dotted curves *5* (almost overlapped by curve *1*) and *6* depict behavior of PS and PI arms in 1,4-dioxane (θ-solvent for PI). The shift of the R_G distribution towards smaller values is very clear for PI because the PI arms are longer and flexible. The PS arms are shorter and they cannot compensate increasing incompatibility penalty by expansion and therefore their distribution almost does not change. However, the snapshots (see the next part) suggest that both types of arms segregate, which results in the formation of pronounced non-centre-spherical conformations. The curves for system S1 are qualitatively similar to those of S2 (not shown).

A comparison of simulated and experimental mean radii of gyration of the whole star for both systems is shown in Table IV. It is evident that experimental and simulated data compare very well at the quantitative level and that the used lattice Monte Carlo simulations are able to reproduce important features of real systems.

The extent of segregation of blocks is not an easily accessible quantity by current experimental techniques, but functions characterizing it can be calculated easily during Monte Carlo simulations. Average distances between the gravity centers of both types of arms, their distribution and distances of individual gravity centers from the center of the star (defined as a small crosslinking core to which the arms are connected) provide the most straightforward description of conformations of an ensemble of segregated heteroarm stars. Figure 2 shows distributions of the latter distances. Full curves *1* and *2* show the distribution of centers of PS and PI, respectively, in a common good solvent (tetrahydrofuran). We would like to point out that

TABLE IV
Comparison of simulated and experimental mean radii of gyration of the whole star, R_G (in nm)

Star copolymer	Experiment THF	Simulation common good solvent	Experiment cyclohexane	Simulation θ-solvent for PS	Experiment 1,4-dioxane	Simulation θ-solvent for PI
S1	19.2	19.1	18.2	18.3	16.5	16.5
S2	26.0	26.2	25.1	25.6	22.7	22.2

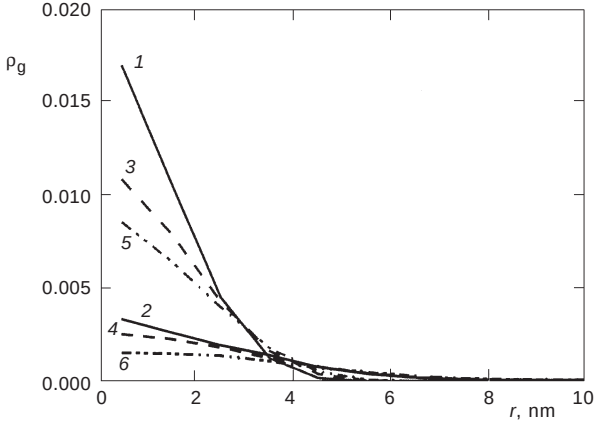

FIG. 2
Distribution functions of distances between the centers of gravity of PS and PI blocks and the geometrical center (the branch point) of the star, $\rho_{T,PS}(r)$ and $\rho_{T,PI}(r)$, respectively, star-(polystyrene; polyisoprene), PS_8PI_8, S2. The numbering of curves is the same as in Fig. 1

it concerns probability densities and the presented functions have to be multiplied by $4\pi r_{CG}{}^2 \Delta r_{CG}$ to get the number fractions of segregated stars with the gravity center of a given arm in a spherical layer of the thickness Δr_{CG} in the distance r_{CG} from the geometrical center. The curve for PS is much higher in the central part than that for PI because the normalization conditions (for PS and similarly for PI) simply reads

$$4\pi \int_0^{r_{max}} \rho_{CG}^{PS}(r_{CG}) r_{CG}^2 \, dr_{CG} = 1 \qquad (6)$$

and PS arms concentrate in the center because their r_{max} (the arm contour length) is shorter. Broken lines *3* and *4* and dotted lines *5* and *6* show corresponding distributions for PS and PI in cyclohexane and in 1,4-dioxane, respectively. The curves describing the distribution of r_{CG} distances in a common good solvent decrease monotonically and steeply with increasing distance. This means that in most stars, the gravity centers of both types of arms overlap with the overall gravity center in the position where the geometrical center is located (the branch point) and the average segregation is negligible. In both selective θ-solvents, probability densities for small r_{CG} decrease and the relative contribution of segregated conformation increases. Curve *6* (corresponding to PI in 1,4-dioxane) levels off for r_{CG} going to zero. Hence we may conclude that segregation increases with decreasing quality of the solvent for one of blocks, i.e., with increasing solvent selectivity.

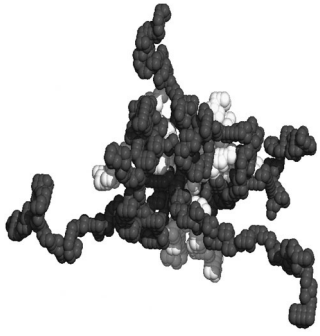

FIG. 3
A typical simulation snapshot of star-(polystyrene; polyisoprene), PS_8PI_8, S2 in a common good solvent. Dark spheres represent PI arms (Monte Carlo segments B), light spheres represent PS arms (Monte Carlo segments A) and shadow areas emulate 3D image.

The conformation behavior can be well documented by typical snapshots. Figure 3 shows a snapshot of the coarse-grained system S2 in a common good solvent. The picture shows a conformation with fairly interpenetrated longer PI and shorter PS arms. Figure 4 shows the same star S2 in a θ-solvent for PS. The short PS arms are parly collapsed and the conformation reminds of a polymer micelle. The last snapshot (Fig. 5) shows a typical heteroarm star conformation in a θ-solvent for long PI arms. In this case, the collapse of long PI arms results in expulsion of PS arms from the

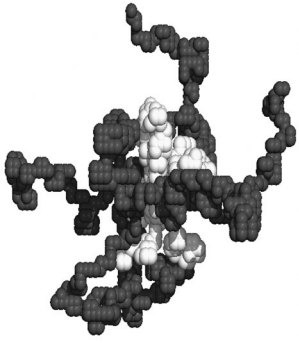

FIG. 4
A typical simulation snapshot of star-(polystyrene; polyisoprene), PS_8PI_8, S2 in the θ-solvent for PS and a good solvent for PI. Dark spheres represent PI arms (Monte Carlo segments B) and light spheres represent PS arms (Monte Carlo segments A)

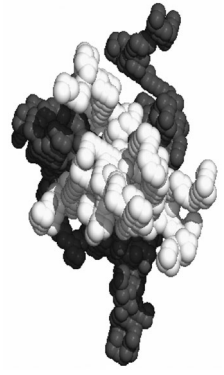

FIG. 5
A typical simulation snapshot of star-(polystyrene; polyisoprene), PS_8PI_8, S2 in the θ-solvent for PI and a good solvent for PS. Dark spheres represent PI arms (Monte Carlo segments B) and light spheres represent PS arms (Monte Carlo segments A)

region rich in PI beads and in formation of a pronounced segregated structure.

CONCLUSIONS

We have shown that relatively simple lattice Monte Carlo simulations are a suitable tool for studying conformations of heteroarm star copolymers in solvents differing in thermodynamic quality for individual blocks. In a common good solvent, their arms are interlaced, but the incompatibility of PS and PI arms results in expansion of the star volume compared with those of corresponding homoarms.

In selective solvents, the worse-soluble arms A shrink and soluble arms B are expelled from the region occupied by concentrated arms A, which results in the formation of a non-spherical segregated conformations.

The observed effects (size changes, tendency to segregate and others) are more pronounced when the thermodynamic quality of the solvent for PI deteriorates, because these arms are longer.

The authors would like to acknowledge financial support of the Grant Agency of the Czech Republic (grant No. 203/03/0262).

REFERENCES

1. Shea J. E., Brooks C. L.: *Annu. Rev. Phys. Chem.* **2001**, *52*, 499.
2. Mitsutake A., Sugita Y., Okamoto Y.: *Biopolymers* **2001**, *60*, 96.
3. Saiz L., Bandyopadhyay S., Klein M. L.: *Biosci. Rep.* **2002**, *22*, 151.
4. Gorbunov A. A., Skvortsov A. M.: *Adv. Colloid. Interface Sci.* **1995**, *62*, 31.
5. Freire J. J.: *Advan. Polym. Sci.* **1999**, *143*, 35.
6. Zifferer G., Petrik T., Neubauer B. O.: *Macromol. Symp.* **2002**, *181*, 331.
7. Genson K. L., Hoffman J., Teng J., Zubarev E. R., Vaknin D., Tsukruk V. V.: *Langmuir* **2004**, *20*, 9044.
8. Binder K., Milchev A.: *J. Comput. Aided Mater. Des.* **2002**, *9*, 33.
9. Groot R. D., Warren P. B.: *J. Chem. Phys.* **1997**, *107*, 4423.
10. Forster S., Konrad M.: *J. Mater. Chem.* **2003**, *13*, 2671.
11. Riess G.: *Prog. Polym. Sci.* **2003**, *28*, 1107.
12. Uhlík F., Limpouchová Z., Jelínek K., Procházka K.: *J. Chem. Phys.* **2004**, *121*, 2367.
13. Limpouchová Z., Procházka K.: *Macromol. Theory Simul.* **2004**, *13*, 328.
14. Havránková J., Limpouchová Z., Procházka K.: *Macromol. Theory Simul.* **2003**, *12*, 512.
15. Jelínek K., Limpouchová Z., Procházka K.: *Macromol. Theory Simul.* **2000**, *9*, 703.
16. Limpouchová Z., Viduna D., Procházka K.: *Macromolecules* **1997**, *30*, 8027.
17. Viduna D., Limpouchová Z., Procházka K.: *Macromolecules* **1997**, *30*, 7263.
18. Procházka K., Limpouchová Z.: *Collect. Czech. Chem. Commun.* **1994**, *59*, 2166.

19. Pispas S., Avgeropoulos A., Hadjichristidis N., Roovers J.: *J. Polym. Sci., Part B: Polym. Phys.* **1999**, *37*, 1329.
20. Voulgaris D., Tsitsilianis C., Grayer V., Esselink F. J., Hadziioannou G.: *Polymer* **1999**, *40*, 5879.
21. Voulgaris D., Tsitsilianis C., Esselink F. J., Hadziioannou G.: *Polymer* **1998**, *39*, 6429.
22. Kiriy A., Gorodyska G., Minko S., Stamm M., Tsitsilianis C.: *Macromolecules* **2003**, *36*, 8704.
23. Siepmann J. I., Frenkel D.: *Mol. Phys.* **1992**, *75*, 59.
24. Rosenbluth M. N., Rosenbluth A. W.: *J. Chem. Phys.* **1955**, *23*, 356.
25. Sokal A. D. in: *Monte-Carlo and Molecular Dynamics Simulation in Polymer Science* (K. Binder, Ed.). Oxford University Press, Oxford, New York 1995.
26. Burchard W in: *Light Scattering Developments and Principles* (E. Brown, Ed.), p. 439. Clarendon Press, Oxford 1996.